Available online at www.sciencedirect.com

ScienceDirect

Underground Space 6 (2021) 1–11

www.elsevier.com/locate/undsp

Evaluation of the propensity of strain burst in brittle granite based on post-peak energy analysis

Selahattin Akdag, Murat Karakus *, Giang D. Nguyen, Abbas Taheri, Thomas Bruning

School of Civil, Environmental and Mining Engineering, The University of Adelaide, Adelaide, SA, Australia

Received 28 February 2019; received in revised form 22 May 2019; accepted 14 August 2019
Available online 11 October 2019

Abstract

The increasing demand for resources and depletion of near ground mineral resources caused deeper mining operations under high-stress rock mass conditions. As a result of this, strain burst, which is the sudden release of stored strain energy in the surrounding rock mass, has become more prevalent and created a considerable threat to workers and construction equipment. It is, therefore, imperative to understand how strain burst mechanism and stored excess strain energy are affected due to the high confinement in deep underground conditions. For this purpose, post-peak energy distributions for brittle rocks were investigated using a newly developed energy calculation method associated with acoustic emission (AE). A series of quasi-static uniaxial and triaxial compression tests controlled by the circumferential expansion were conducted. Snap-back behaviour known as Class-II behaviour associated with energy evolution and the material response under self-sustaining failure were analysed on granites under a wide range of confining pressures (0–60 MPa). The experimental results underline that the energy evolution characteristics are strongly linked to confinement. Stored elastic strain energy (dU_E), energy consumed by dominating cohesion weakening ($d\Phi_{CW}$) and energy dissipated during mobilisation of frictional failure ($d\Phi_{FM}$) showed a rising trend as the confining pressure was increased. An intrinsic ejection velocity was proposed to express the propensity of strain burst that was purely determined by the excess strain energy released from Class II rock.

Keywords: Strain burst; Energy balance; Class II failure mode; Self-sustaining failure; Triaxial compression test; Circumferential strain control

1 Introduction

Strain burst is a dynamic rock failure in deep underground excavations that is characterised by a sudden and/or violent ejection of rock fragments at a certain speed. Due to the nature of unpredictability, strain burst has become a most serious threat for people and the production in deep underground operations. Thus an in-depth understanding of the failure mechanism of strain burst is of utmost significance for prediction, mitigation, and control of strain burst in deep underground mining and engineering projects.

The magnitude of strain burst, the amount of kinetic energy released, the volume of ejected rock, and the ejection velocity and degree of rock fragmentation can show a considerable variation due to the mineral composition of the brittle rocks. The manifestation of strain burst is related to the elastic stored strain energy and how this stored energy is released during unstable spontaneous failure (Bruning, Karakus, Nguyen, & Goodchild, 2018b; Tarasov & Potvin, 2013). The first law of thermodynamics states that the energy transformation process of strain burst in rock mass involves energy storage, dissipation, and release. Hence, it is significant to investigate the energy state during strain burst from the viewpoint of energy theory. Indeed, the failure of rock is driven by energy activities, including absorption, evolution, dissipation,

* Corresponding author.
E-mail address: murat.karakus@adelaide.edu.au (M. Karakus).

https://doi.org/10.1016/j.undsp.2019.08.002

and the release of strain energy (Huang & Li, 2014; Li, Sun, Xie, Li, & Ranjith, 2017; Peng et al., 2015; Weng, Huang, Taheri, & Li, 2017; Zhou, Xu, Karakus, & Shen, 2019). Over the last few decades, extensive relevant researches have been conducted to gain a better understanding of the mechanism of strain burst and the energy evolution using laboratory tests (Bruning, Karakus, Akdag, Nguyen, & Goodchild, 2018a; Hauquin, Gunzburger, & Deck, 2018; He, Jia, Coli, Livi, & Sousa, 2012; Hua & You, 2001; Li, Du, & Li, 2015; Meng, Zhang, Han, Pu, & Nie, 2016; Xu & Karakus, 2018). Li, Huang, and Li (2014) studied the strain rate dependency of rock strength, deformation and strain energy conversion. It has been proven that absorbed strain energy and elastic strain energy increase with strain rate, and a greater amount of stored elastic strain energy in the specimen generates stronger fragmentation. Peng et al. (2015) analysed the energy dissipation and release characteristics during coal failure by conventional triaxial compression, and proposed two parameters based on energy analysis to describe the failure mode of coal under various confining pressures. To investigate energy evolution characteristics of granite specimens in triaxial deformation, Li et al. (2017) carried out triaxial tests with different loading and unloading stress paths, including microscopic analysis of rock failure fracture. They found that the ratio of the dissipated strain energy to the total strain energy is a good indicator of rock deformation process and it initially increases, and later decreases to almost a plateau, and finally increases rapidly, which corresponds to the deformation stages of rock under triaxial compression. Ning et al. (2018) introduced a new energy-dissipation method based on energy theory to identify crack initiation and crack damage thresholds. They reported that the crack initiation threshold and crack damage stress can be quantified by obtaining the pre-peak dissipated energy ratio. These efforts have enriched the knowledge of the energy evolution mechanism of rocks under various loading conditions. Nevertheless, the studies above did not consider the effects of confinement on the energy evolution characteristics in the post-peak stage that occur during strain burst failure process. Therefore, it is necessary to intensively investigate the role of energy redistribution in strain burst and how it is influenced with confining pressure. In this sense, complete stress–strain characteristics of intact rock, i.e. the pre-peak and post-peak stress–strain regimes, are crucial in understanding and interpreting the process of rock deformation and failure.

It is well understood that the stress–strain behaviour of rock is the external manifestation of energy evolution during deformation and failure. Therefore, the complete stress–strain response of rock, importantly post-peak failure stage, is the fundamental information to describe the processes of energy redistribution, evolution and rock deformation as strain burst takes place at the post-peak failure stage. Numerous relevant attempts have been made by researchers to obtain the full stress–strain response of rock in compression by controlling the application of load through a feedback of axial load (Bieniawski & Bernede, 1979), axial displacement (Gowd & Rummel, 1980), or axial strain rate (Okubo, Nishimatsu, & He, 1990). However, these control methods are only sufficient to measure pre-peak behaviour, not to capture post-peak stage of Class II rocks which is characterised by a strong strain localisation as axial strain no longer monotonically increases from the moment that rock exhibits Class II behaviour (Munoz & Taheri, 2017). In this sense, the circumferential- or lateral-strain controlled method is more appropriate to measure the post-peak stress–strain response for brittle rocks (Fairhurst & Hudson, 1999; Munoz, Taheri, & Chanda, 2016; Wawersik & Fairhurst, 1970). In this study, full stress–strain behaviour and energy evolution characteristics of brittle rock were analysed by performing uniaxial and triaxial compression tests by controlling the application of load through a feedback loop of circumferential strain. Rocks exhibiting Class II behaviour undergo self-sustaining fracturing due to excess stored strain energy which is accompanied by some energy release. Hence, principles of the energy redistribution during strain burst, in some regards, can be compared with principles involved in the spontaneous failure of Class II, which implies that the role of energy in strain burst can be better understood by analysing the energy characteristics of rock in compression.

In the present study, the effects of confining pressure on the evolution of strain energy during strain burst of Class II rocks were analysed by using an energy-based approach taking into account the snap-back behaviour. A series of circumferential strain controlled quasi-static uniaxial and triaxial compression tests were conducted on granite specimens over the confining pressure varying from 0 to 60 MPa to capture the snap-back behaviour and calculate stored strain energy, dissipated energy, and excess strain energy responsible for the spontaneous instability. An energy calculation methodology based on the post-peak energy analysis was developed to describe the propensity of strain burst and the effects of confining pressure on energy characteristics at the post-peak failure stage were also analysed.

2 Experimental methodology

Experimental work includes the investigation of the confinement influence on the propensity of strain burst of rocks exhibiting Class II behaviour under varying confining pressures. The main objective of this study was to quantitatively estimate the energy redistribution characteristics of brittle rock based on a newly developed energy calculation method, conducting circumferential strain control uniaxial and triaxial compression tests. Two groups of tests were carried out in this study: Group (1) was the circumferential strain controlled uniaxial compression tests to quantitatively examine the potential intensity of strain burst, and Group (2) was the circumferential strain controlled tri-

axial compression tests to develop a new energy calculation method based on the post-peak energy balance of snap-back behaviour and investigate the influence of confinement on the post-peak energy evolution characteristics.

2.1 Rock material and preparation

The granite specimens were collected from a borehole located in South Australia at depth ranging from 1020 m to 1345 m. The grain size of the granite varies between 0.5 and 3 mm within a coarse-grained matrix. The granite selected for testing mainly comprised of quartz, feldspar, chlorite and potassium.

The granite specimens were sub-cored from 63 mm diameter drill cores and cut using diamond coring and cutting apparatus to obtain cylindrical samples of 42 mm in diameter and 100 mm in length in which the aspect ratio (i.e. length to diameter ratio) was maintained at 2.4 (Fairhurst & Hudson, 1999). The diameter of the specimens was more than 20 times bigger than the rock grain size satisfying International Society for Rock Mechanics (ISRM) recommendations (Fairhurst & Hudson, 1999). Both ends of the specimens were then finely ground flat and parallel to each other within approximately 0.01 mm and polished to minimise the end effect during loading. The average uniaxial compressive strength (UCS) of the granite samples is 158 MPa with a density of 2871 kg/m^3, the average elastic modulus is 38.6 GPa, and the average P-wave velocity of the specimens is 5764 m/s.

2.2 Circumferential strain controlled uniaxial and triaxial compression tests

A series of uniaxial compression tests were carried out on Australian granite. Compression tests were compiled with circumferential-strain controlled method in order to capture the post-peak response of rock. The rock samples were subjected to a quasi-static monotonic axial loading by a closed-loop servo-controlled Instron 1282 hydraulic compression machine, with a loading capacity of 1000 kN, which was stiff enough not to allow the elastic energy accumulated in the machine (see Fig. 1). The applied axial load was initially controlled at an axial-strain feedback at a rate of 0.001 mm/mm/s until reaching approximately 70% of the expected peak force ($0.7F_{peak}$) and then the control mode was switched to circumferential control, in a way keeping lateral-strain rate constant by the circumferential extensometer outlined in the ISRM method (Fairhurst & Hudson, 1999).

A granite specimen was instrumented by a pair of strain gauges (30 mm in length) oriented in the axial direction to measure the corresponding axial strain, ε_a. Additionally, the vertical displacement of the granite specimens was measured externally by a pair of linear variable differential transformers (LVDTs), which were mounted on both sides of the specimens. Besides, direct-contact lateral ring-shaped extensometer was mounted along the perimeter and at the mid-length of the specimens which eliminated the end-edge friction influence. This setup was used to both control the axial load by lateral-strain feedback and record lateral strain, ε_l.

To reveal the influence of confinement on rock energy evolution characteristics, and post-peak energy distribution of Class II behaviour under self-sustaining failure, a number of granite specimens were also tested under six confining stresses, 10, 20, 30, 40, 50 and 60 MPa. A closed-loop servo-controlled Instron 1282 load system was used as a testing frame to carry out triaxial compression tests. A Hoek cell with a capacity up to 65 MPa was used to apply confining pressure in these tests. Circumferential strain control was utilised by means of a Hoek cell membrane fitted with four strain gauges internally within the cell, as depicted in Fig. 1. More details can be found in Bruning, Karakus, et al. (2018b). The circumferential strain control method suggested by ISRM for obtaining the complete stress–strain curve was adopted in these tests. The specimen was loaded axially with a constant growth of circumferential strain of 1×10^{-6} mm/mm/s. The first step of the test was to apply a hydrostatic pressure on the rock specimen until the pressure reached the required magnitude of the confinement. After that, the axial loading was applied using the circumferential strain control method while keeping the confining stress constant.

2.3 Acoustic emission measurement

The Acoustic emission detection technology is a powerful non-destructive technique to investigate the failure process and crack evolution mechanism in brittle rocks (Lockner, 1993). When a brittle rock is under stress, strain energy is released during the development of new cracks or the widening of existing cracks. This energy is released in the form of elastic waves from the crack tips, and can be captured and amplified by an AE system. Therefore, AE detection technique has been widely used in a number of previous researches to study the crack development mechanism in brittle rocks (Carpinteri et al., 2013; Karakus, Akdag, & Bruning, 2016; Akdag, Karakus, Taheri, Nguyen, & Manchao, 2018; Bruning, Karakus, et al., 2018b; Weng, Li, Taheri, Wu, & Xie, 2018). During experiments, in order to analyse fracturing characteristics, and damage evolution mechanism of the granite specimens, the output of AEs was continuously monitored. It is known that acoustic emission can be defined as the transient elastic waves induced by the rapid release of localised energy due to crack formation and propagation within a material (Akdag et al., 2018; Bruning, Karakus, et al., 2018a; Carpinteri et al., 2013; Karakus et al., 2016). In the present study, the AE system was started simultaneously with the loading and the pre-amplifiers of two AE sensors were set to 60 dB (Type 2/4/6) to amplify the AE signals during loading. The resonance frequency of the AE transducers was 125 kHz, associated with an operating frequency rang-

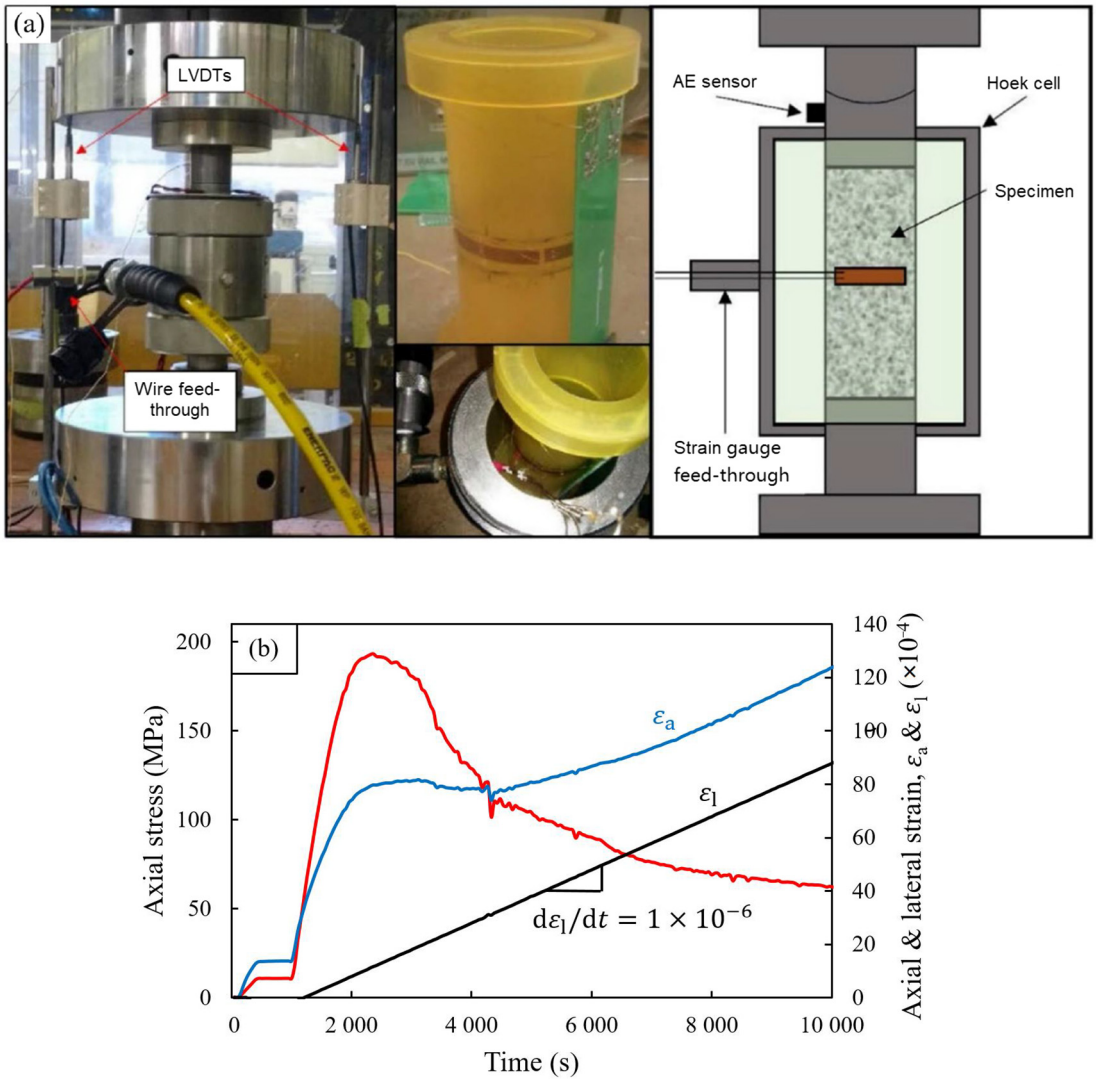

Fig. 1. (a) Testing setup for circumferential controlled triaxial compression tests and strain gauged membrane (Bruning, Karakus, et al., 2018b) and (b) typical time history of a loading and strains in circumferential-strain control feedback triaxial compression test in the present study.

ing from 100 kHz to 1 MHz. A PCI-2 AE system was used to monitor the damage within the granite specimens during compression tests, and the sampling rate was set to 2 MS/s. The amplitude threshold for AE detection was set to 45 dB to ensure environmental noise was no longer registered during data acquisition.

3 Evaluation of the experimental results

3.1 New energy calculation method based on the post-peak energy balance of snap-back behaviour

The stress–strain response is the phenomenological manifestation of the energy evolution during rock failure. Under compression, the stress–strain curves of the post-peak behaviour of rocks can be classified as Class I and II. Class I behaviour is characterised by a negative post-peak slope which means that loading must be applied to generate additional energy for maintaining the entire fracture process until the failure of the rock occurs. Class II rock behaviour, on the other hand, shows a positive post-peak slope and the elastic stored strain energy in the rock specimen is sufficient to display self-sustaining failure which is accompanied by some energy release. The post-peak behaviour is a reflection of some intrinsic material properties which allows estimating the dynamic energy balance at spontaneous failure. Therefore, full stress–strain behaviours of rock undergoing uniaxial and triaxial compression play a significant role to describe the total energy evolution and rock deformation. In this respect, the full stress–strain and the post-peak characteristics of hard brittle granite samples exhibiting Class II behaviour under uniaxial and triaxial compression, which can be compared with the stress state of a strain burst, were obtained by utilising the circumferential-strain controlled loading method.

Figure 2 shows the full stress–strain curve of a granite tested at a confinement of 10 MPa. Area of the green triangle (dU_E) corresponds to the elastic stored strain energy

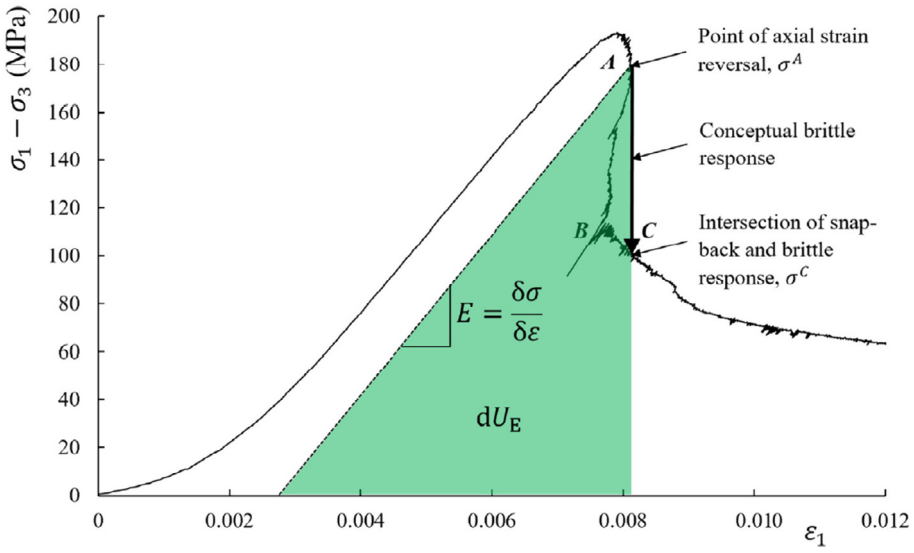

Fig. 2. Class II behaviour and elastic stored strain energy of granite under 10 MPa confinement.

within the specimen before it displays 'snap-back' behaviour, which is the energy source for fracturing and spontaneous failure (strain burst).

Tarasov and Potvin (2013) assessed rock brittleness under triaxial compression and established a corresponding brittleness index based on the energy balance of the post-peak stage of full stress–strain curve. However, this energy calculation framework did not take into account the energy dissipation due to cohesion loss and frictional failure and the excess strain energy released during brittle failure (bursting). Herein, we propose a new energy calculation method to investigate the post-peak regime of rocks exhibiting Class II behaviour. Using the AE characteristics during compression tests, fracture energy was split into two-classes: (1) energy consumed due to gradual loss of dominating cohesive behaviour and (2) energy dissipated during the mobilisation of frictional failure (as shown in Fig. 3). In Fig. 3, blue and yellow areas represent the energy consumed by cohesion weakening during stable fracturing ($d\Phi_{CW}$) and the energy dissipated during the mobilising frictional sliding ($d\Phi_{FM}$), respectively. The green area is corresponding to the residual stored elastic strain energy ($d\Phi_{RE}$). For Class II rock behaviour, the elastic strain energy accumulated within the rock is sufficient to maintain the entire failure of the rock which indicates that rocks exhibiting snap-back behaviour are close to absolute brittleness. In this case, self-sustaining fracturing forces rock into failure, which is accompanied by some energy release. The red area (subtended by snap-back part) represents the excess strain energy released during brittle failure

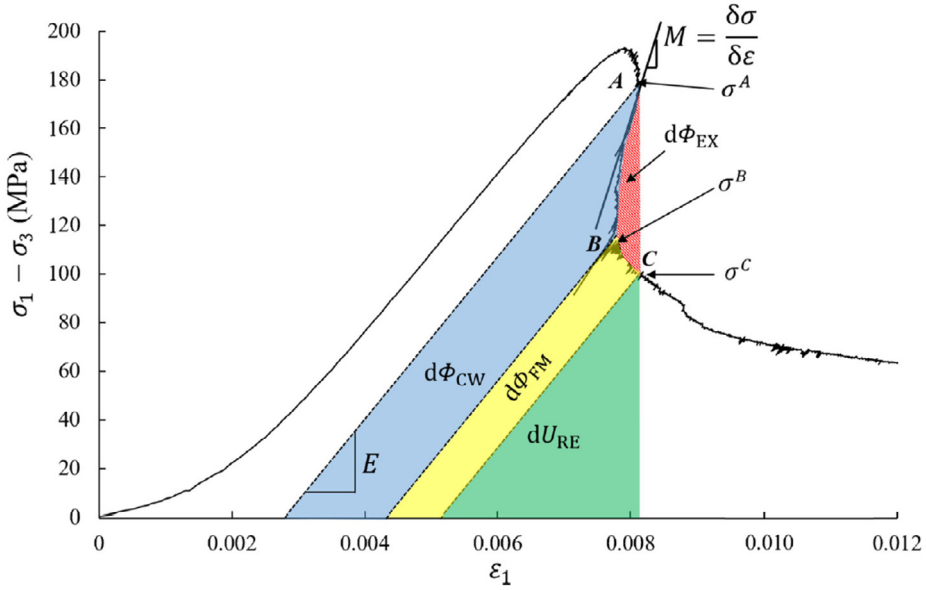

Fig. 3. Schematic diagrams of energy calculation during Class II behaviour of granite under 10 MPa confinement.

(energy in excess, $d\Phi_{EX}$) which is responsible for the intrinsic potential energy for strain burst in the rock. The above assumptions on unloading without stiffness change and different stages of failure based on the measured macro behaviour facilitate the calculation of energies in this study. We are aware that they may not always truly reflect the underlying failure modes that are a combination of microcracking and friction between microcrack surfaces. The links between macro behaviour and underlying microstructural processes require advanced experimental techniques that can track the evolution of these processes in real time, given the very fast failure in rocks under uniaxial/triaxial compression condition. This is beyond the scope of this study.

The Class II failure process between points A and C can be characterised by the following types of specific (per unit volume) energy calculations (Eqs. (1)–(5)):

$$dU_E = \frac{(\sigma^A)^2}{2E}, \tag{1}$$

$$d\Phi_{CW} = \sum_{i=A}^{B} \frac{(\sigma^i)^2 - (\sigma^{i+1})^2(M-E)}{2EM}, \tag{2}$$

$$d\Phi_{FM} = \sum_{i=B}^{C} \frac{(\sigma^i)^2 - (\sigma^{i+1})^2(M-E)}{2EM}, \tag{3}$$

$$dU_{RE} = \frac{(\sigma^C)^2}{2E}, \tag{4}$$

$$d\Phi_{EX} = dU_E - d\Phi_{CW} - d\Phi_{FM} - dU_{RE}, \tag{5}$$

where U_E is the elastic stored strain energy after the point of Class II behaviour, Φ_{CW} is the energy consumption dominated by cohesion degradation during stable fracturing, Φ_{FM} is the energy dissipated during the mobilisation of frictional failure, U_{RE} is the residual stored elastic strain energy, Φ_{EX} is the excess strain energy released during brittle failure (bursting), σ^A is the point of axial strain reversal, σ^B is the point of brittle failure intersection, E is the elastic stiffness of the specimen and M ($M = \delta\sigma/\delta\varepsilon$) is the post-peak modulus between two incremental stress points.

In this study, the AE technique was adopted to assess the post-peak energy evolution characteristics of the granite specimens under various confining pressures. Figure 4 shows axial stress–strain and AE hits characteristics for rocks with Class II behaviour tested in triaxial compression ($\sigma_3 = 10$ MPa). From near peak (pre-peak) to the point of axial strain reversal (σ^A), some microcracking is mobilised that facilitates fracture process, e.g. creating more surfaces

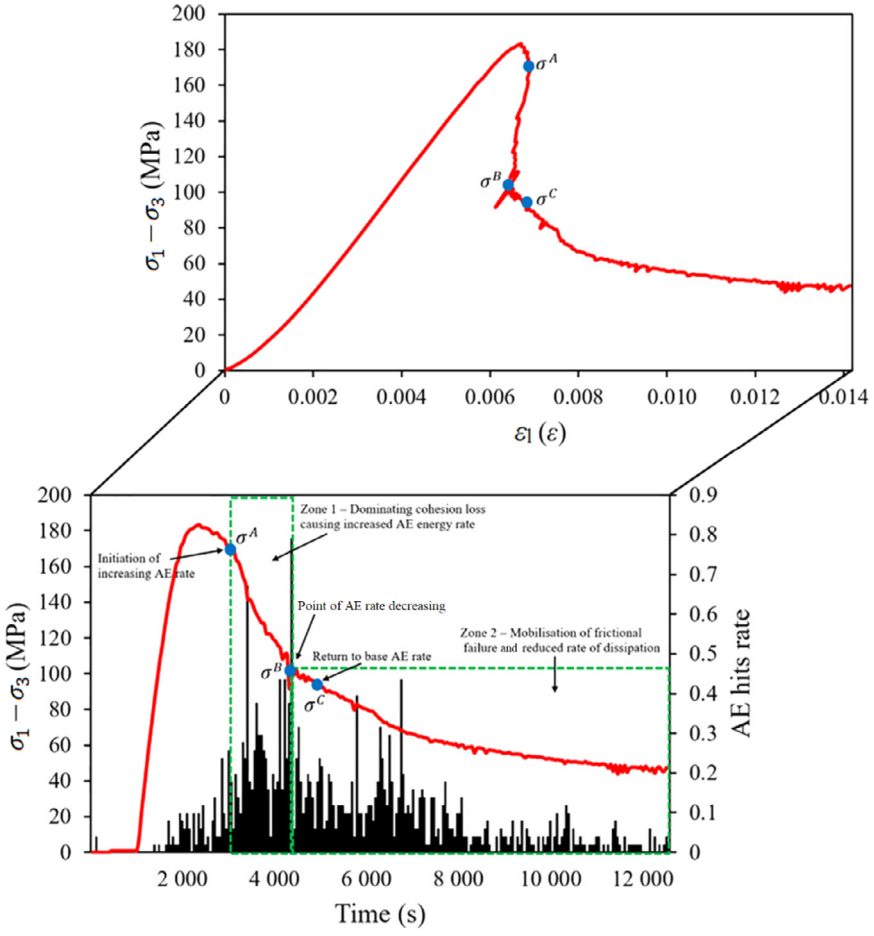

Fig. 4. Stress–strain and AE energy characteristics for Class II rock under 10 MPa confinement.

to facilitate sliding. In Zone (1), the energy dissipation of the rock specimen is provided by the initiation and further opening of microcracks in the specimen. In this energy dissipation process, cohesion degradation and frictional sliding facilitates simultaneously in which cohesion weakening is dominant, but the energy needed to further fail the specimen is below the storage. During this process, further degradation of cohesive strength leads to more fracture surface created and hence gradually shows stronger interlocking. This is typified by the increasing AE activities as more microcracks are opened. Once a certain level of microcrack generation is reached, the fractures start to coalesce and propagate forming macrocracks (Zone 2). This allows frictional sliding to dominate the fracture energy dissipation process. More energy is gradually required to further fail the specimen, due to friction strengthening and also lower energy storage. At this stage the sliding plane has formed in rock and a more constant rate of AE energy is recorded. Therefore, with fracture propagation, dominating cohesion loss (Zone 1) is gradually substituted by the mobilisation of frictional failure (Zone 2) which is accompanied by the decrease in bearing capacity of the specimen from the cohesive strength to the frictional (residual) strength (Bazant, 1996; Bruning, Karakus, Nguyen, & Goodchild, 2019; Landis, Nagy, & Keane, 2003; Munoz & Taheri, 2019; Remani & Martin, 2018; Tarasov & Potvin, 2013). This new method for determining the energy dissipation of compressive tests avoids the grouping of all energy into the term 'energy lost due to stable fracturing'. This is significant when considering phenomena like strain burst, since frictional processes are not likely to occur at the excavation face due to the sudden ejection of rock fragments and spalling type of failure. Therefore, these energy measures can be further studied to determine their role in strain burst prediction and mechanism investigation.

3.2 Influence of confining pressure on the energy balance of Class II at spontaneous failure

The release of excess strain energy and the increase of dissipated fracture energy caused a reduction in the energy storage capacity of the rock so that rock deformation increased gradually and tended to fail. The formation of macrocracks and failure surfaces in the rock promoted the conversion of the accumulated elastic strain energy into the forms of energy to be dissipated and released which resulted in spontaneous bursting. Due to the aggravation of dramatic internal fracture expansion, further strength loss took place with a transition into the residual stage in which some amount of strain energy was stored within the specimen (see Fig. 3).

Figure 5 shows axial stress–strain and AE hits characteristics for each confinement level. The influences of confinement on the elastic stored strain energy, the energy consumed by dominating cohesion weakening, the energy dissipated during mobilisation of frictional failure and the excess strain energy of the granite specimens are depicted in Fig. 6. It can be seen that the energy redistribution characteristics and material behaviour of Australian granite under different levels of confinement are strongly dependent on confining pressure. When the confining pressure increased to 60 MPa, elastic stored strain energy, and the energy consumed by dominating cohesion weakening, energy dissipated during mobilisation of frictional sliding were 8.74, 2.53 and 12.1 times the values at unconfined condition indicating that the elastic energy accumulates more rapidly as the depth of an underground excavation rises up, resulting in a more severe strain burst (see Figs. 6(a)–(c)). At the pre-peak stage, the growth of the accumulated elastic strain energy was faster than the dissipated energy, indicating that the energy evolution behaviour of granite prior to the onset of 'snap-back' behaviour was mainly dominated by the elastic energy accumulation. This phenomenon implies that the ability of granite specimens to store elastic strain energy was enhanced by the higher confining pressure. In the post-peak regime, the accumulation of elastic energy began to slow down and ultimately became stable and the dissipated fracture energy increased by the development and further openings of microcracks leading to internal damage of rock progressively with a loss of cohesive strength. The expansion, coalescence and propagation of microcracks to form macrocracks led frictional failure to dominate the fracture energy dissipation process in which the sliding plane was formed. The excess strain energy diminished by 46% as the confining pressure increased up to 60 MPa, as depicted in Fig. 6(d). As rising the level of confinement, the frictional strength component was easily mobilised, which caused an increase in frictional resistance to crack propagation. Thus, greater dissipated energy consumption is required to promote crack propagation, revealing that the damage of deep granite is more severe from the viewpoint of energy evolution.

The stress–strain curves of granite under various levels of confinement are shown in Fig. 7(a). The cumulative AE energy-time responses for each confinement are presented in Fig. 7(b) and it can be seen that lateral pressure increases the rate of AE signals, which corresponds to the damage evolution of the rock becoming more gradual. When confining pressure increases the AE emissions occur more gradually with increasing axial strain. This is corresponding to the damage evolution process becoming slower due to the increasing degrees of opposing stress imparted by confinement. In other words, the hardening and more gradual softening behaviour of rock under high confining pressure corresponds to the rate of mirocrack initiation, propagation and coalescence competing against the consolidation effect of lateral pressure.

The failure modes of the granite specimens in triaxial compression are depicted in Fig. 8. The main feature is the multiple longitudinal splitting failure pattern accompanied by local shear failure when $\sigma_3 = 0$ MPa. The formation of extension cracks oriented in the direction of

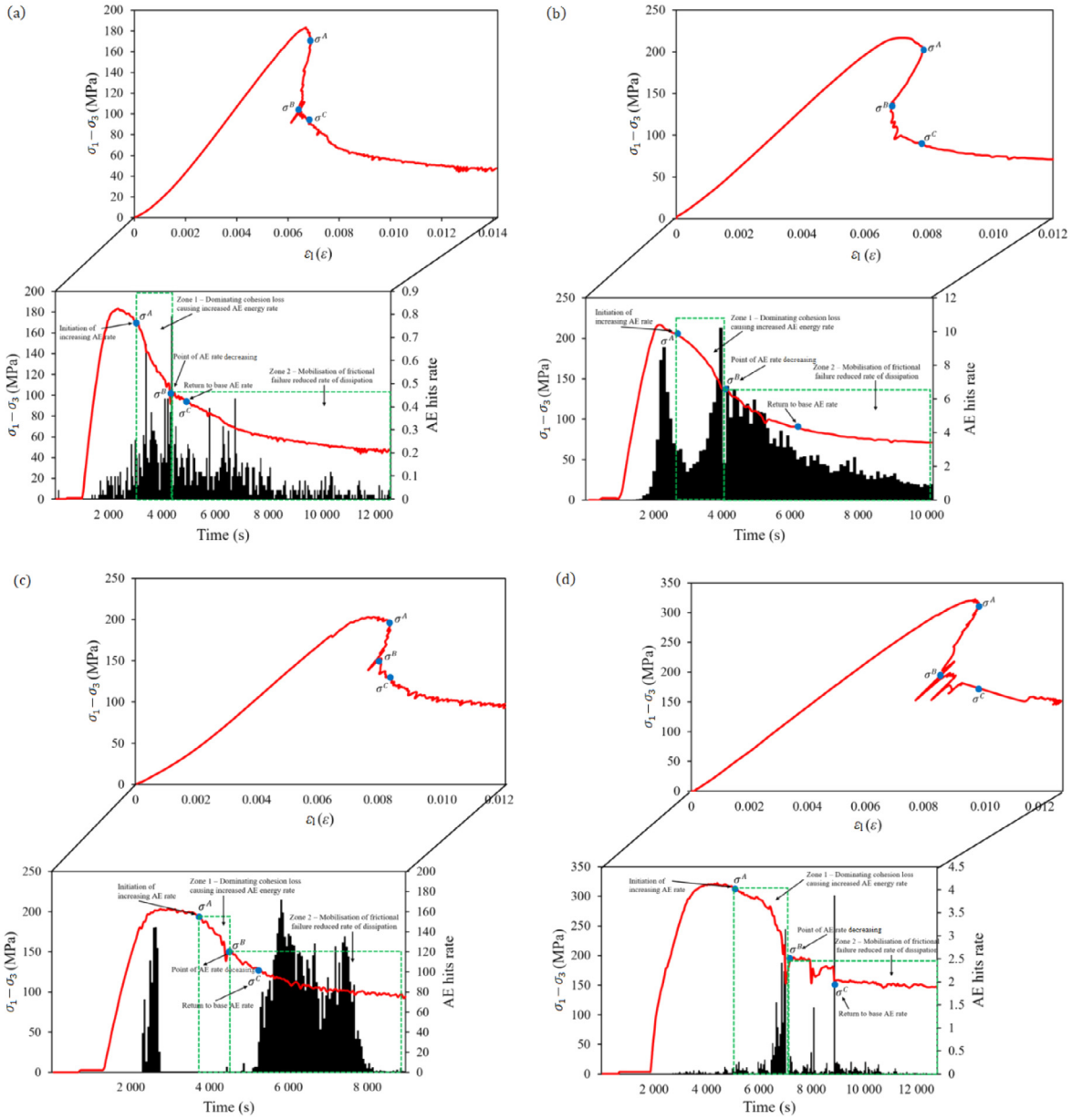

Fig. 5. Stress–strain and AE energy characteristics for Class II rocks under different levels of confinement: (a) $\sigma_3 = 10$ MPa, (b) $\sigma_3 = 20$ MPa, (c) $\sigma_3 = 30$ MPa, (d) $\sigma_3 = 40$ MPa, (e) $\sigma_3 = 50$ MPa, and (f) $\sigma_3 = 60$ MPa.

principal stress is the prevailing pattern of macroscopic fracturing in uniaxial compression. Dominant failure pattern of granite changes to shear failure accompanied by a few short longitudinal splitting cracks with rising confining pressure, as depicted in Fig. 8. Confining pressure restricts the propagation and coalescence of longitudinal cracks, and is beneficial to the expansion of the inclined cracks which are at an angle to the direction of the major principal stress, hence the failure mode changes. The longitudinal splitting crack is a type of tensile crack, which is easily opened and has a small displacement between crack surfaces. Therefore, the dissipated energy needed to initiate and propagate the longitudinal spitting cracks is small. However, granite specimens will slide along the fracture surfaces after the shear failure of the granite specimen under a high confining pressure. This process requires the testing apparatus to provide more energy to overcome the friction and maintain the propagation of the macrocracks.

Another parameter to quantitatively express the potential intensity of a burst event is the ejection velocity of rock fragments (Akdag et al., 2018). The intrinsic ejection velocity, denoted as v, refers to the velocity of rock ejection in a burst event, which is caused by the excess strain energy Φ_{EX} released from the ejected rock fragment. Assuming that the excess strain energy is completely converted to kinetic energy to eject the rock fragments, we obtained the following expression for the ejection velocity:

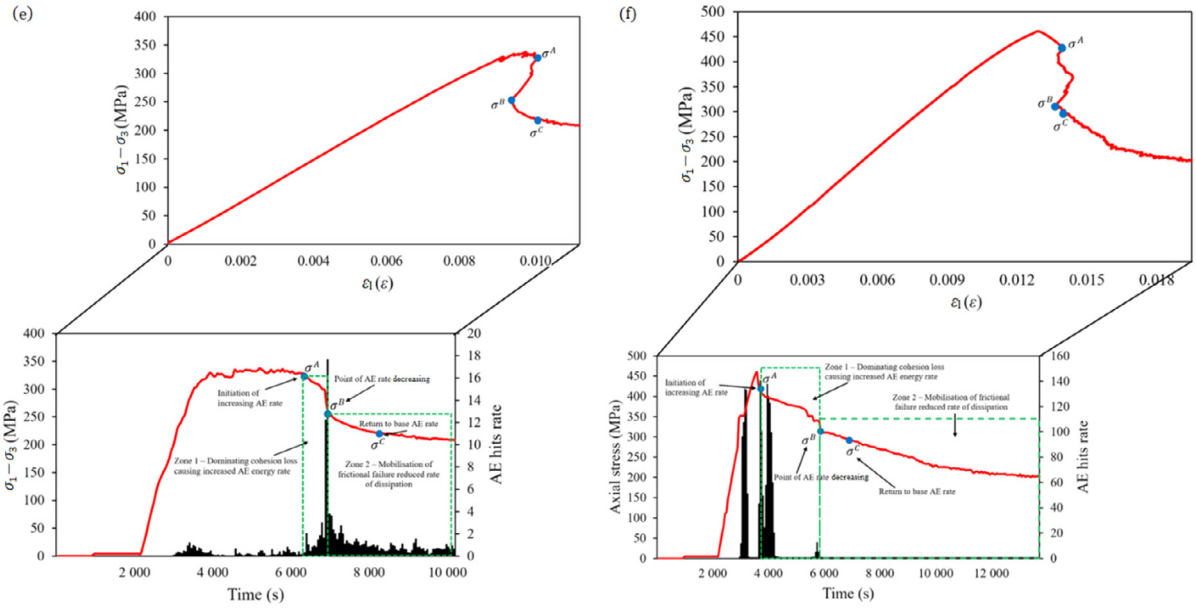

Fig 5. *(continued)*

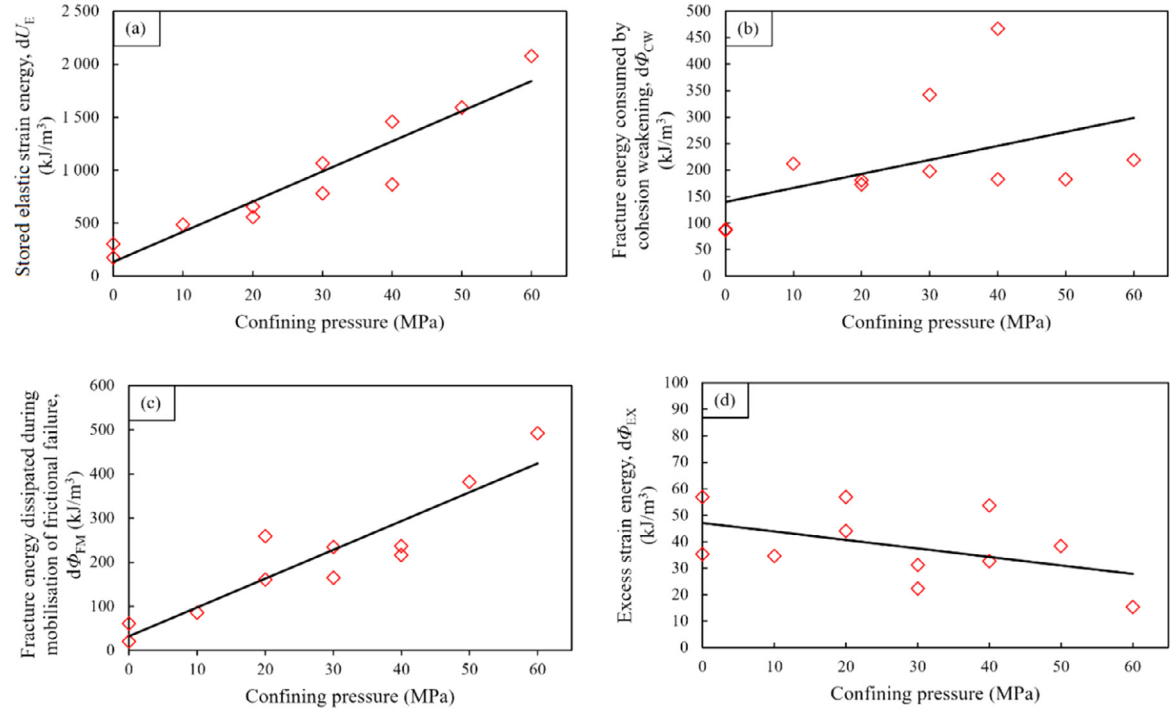

Fig. 6. Variation of (a) Elastic stored strain energy, (b) Energy consumed by dominating cohesion weakening, (c) Energy dissipated during mobilisation of frictional sliding, and (d) Excess strain energy.

$$v = \sqrt{\frac{2}{\rho}\Phi_{EX}}, \tag{6}$$

where v is in m/s, Φ_{EX} is in kJ/m^3 and ρ is the density of the rock in kg/m^3.

The intrinsic ejection velocities of the Australian granite were 6.5 m/s to 5.1 m/s and these values are consistent with those stated by Jiang et al. (2015) and Akdag et al. (2018) in which the ejection velocity of rock fragments were calculated with the help of high-speed cameras.

4 Conclusion

In this study, a series of uniaxial and triaxial compression tests were conducted using circumferential strain control on Class II rocks under different levels of confinement.

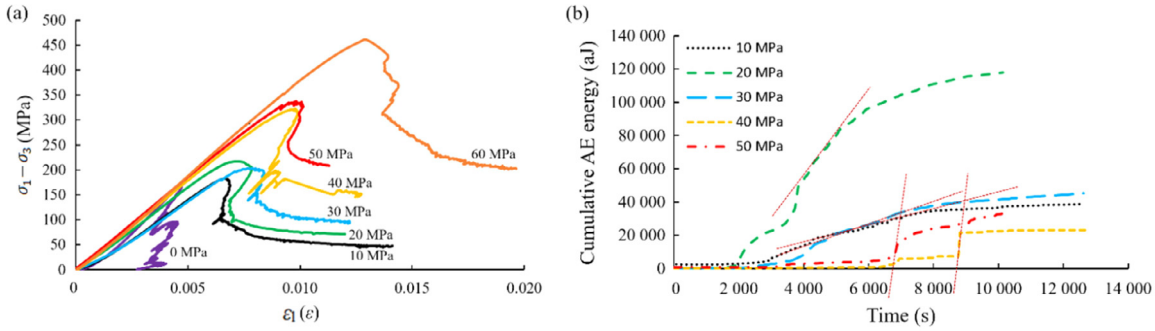

Fig. 7. (a) stress–strain curves and (b) Accumulated AE energy-time curves of the granite specimens under different levels of confinement.

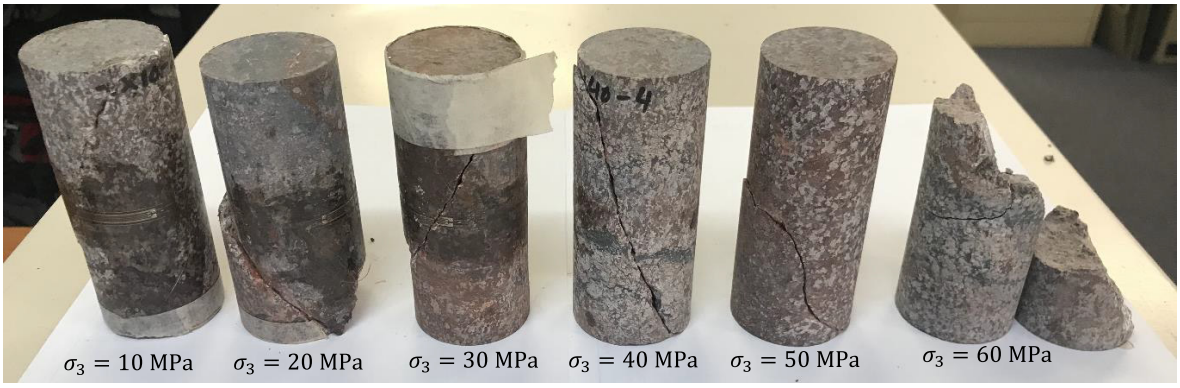

Fig. 8. Fracture patterns of granite specimens under different confining pressures.

Energy evolution, failure and fracture characteristics of the Australian granite at various confining pressures were systematically investigated. The influence of confining pressure on the evolution of strain energy during strain burst of Class II rocks was analysed and the underlying mechanism was discussed. The following important conclusions can be drawn:

(1) An energy calculation method was developed based on the post-peak energy analysis. AE responses during compression tests were used to assess the energy and crack evolution characteristics of Australian granite specimens under different confinement. Using AE characteristics, fracture energy was split into two-class: (i) energy consumed dominantly by gradual weakening of cohesive behaviour and (ii) energy dissipated during the mobilisation of frictional failure. A portion of elastic energy, released from the Class II rock, was defined as excess strain energy which is a measure for the propensity of the intrinsic strain burst in the rock. It directly determines the intrinsic ejection velocity of the rock fragments when a bursting event occurs.

(2) Confinement has significantly affected the post-peak energy redistribution characteristics and fracture mechanism of granite. The elastic stored strain energy, energy consumed by dominating cohesion weakening, and energy dissipated during mobilisation of frictional failure were 8.74, 2.53 and 12.1 times the values at unconfined condition, resulting in more severe strain burst indicating that rising up the confining pressure improved the efficiency of energy accumulation. This explains why the damage degree of deep granite is more prominent in the process of deep excavations. Another parameter to express the intensity of a burst event, the ejection velocity, was calculated as 6.5 m/s and 5.1 m/s, which was consistent with the existing literature. The proposed approach can provide an early warning of brittle rock instability, which is significant for strain burst assessment in deep mining operations.

(3) The fracturing mechanism of granite was influenced by confining pressure. The dominant failure pattern of granite changed from multiple splitting failure to splitting-shear composite failure as the level of confinement increased.

Acknowledgements

The authors gratefully acknowledge the financial support from the Australian Research Council (ARC) (ARC-LP150100539), OZ Minerals, and the principal geotechnical manager David Goodchild. The authors also

wish to thank the laboratory technicians Adam Ryntjes and Simon Golding.

Declaration of Competing Interest

The authors declare no conflicts of interest.

References

Akdag, S., Karakus, M., Taheri, A., Nguyen, G., & Manchao, H. (2018). Effects of thermal damage on strain burst mechanism for brittle rocks under true-triaxial loading conditions. *Rock Mechanics and Rock Engineering, 51*(6), 1657–1682.

Bazant, Z. (1996). Analysis of work-of-fracture method for measuring fracture energy of concrete. *Journal of Engineering Mechanics, 122*(2), 138–144.

Bieniawski, Z., & Bernede, M. (1979). Suggested methods for determining the uniaxial compressive strength and deformability of rock materials: Part 1. Suggested method for determination of the uniaxial compressive strength of rock materials. *International Journal of Rock Mechanics and Mining Sciences & Geomechanics Abstracts, 16*, 137–138.

Bruning, T., Karakus, M., Akdag, S., Nguyen, G., & Goodchild, D. (2018a). Influence of deviatoric stress on rockburst occurrence: An experimental study. *International Journal of Mining Science and Technology, 28*, 763–766.

Bruning, T., Karakus, M., Nguyen, G., & Goodchild, D. (2018b). Experimental study on the damage evolution of brittle rock under triaxial confinement with full circumferential strain control. *Rock Mechanics and Rock Engineering, 51*(11), 3321–3341.

Bruning, T., Karakus, M., Nguyen, G., & Goodchild, D. (2019). An experimental and theoretical stress-strain damage correlation procedure for constitutive modelling of granite. *International Journal of Rock Mechanics and Mining Sciences, 16*, 1–12.

Carpinteri, A., Lacidogna, G., Accornero, F., Mpalaskas, A., Matikas, T., & Aggelis, D. (2013). Influence of damage in the acoustic emission parameters. *Cement and Concrete Composites, 44*, 9–16.

Fairhurst, C., & Hudson, J. (1999). Draf ISRM suggested method for the complete stress-strain curve for intact rock in uniaxial compression. *International Journal of Rock Mechanics and Mining Sciences, 36*, 279–289.

Gowd, T., & Rummel, F. (1980). Effect of confining pressure on the fracture behaviour of a porous rock. *International Journal of Rock Mechanics and Mining Sciences & Geomechanics Abstracts, 17*(4), 225–229.

Hauquin, T., Gunzburger, Y., & Deck, O. (2018). Predicting pillar burst by an explicit modelling of kinetic energy. *International Journal of Rock Mechanics and Mining Sciences, 107*, 159–171.

He, M., Jia, X., Coli, M., Livi, E., & Sousa, L. (2012). Experimental study of rockbursts in underground quarrying of Carrara marble. *International Journal of Rock Mechanics and Mining Sciences, 52*, 1–8.

Hua, A., & You, M. (2001). Rock failure due to energy release during unloading and application to underground rock burst control. *Tunnelling and Underground Space Technology, 16*(3), 241–246.

Huang, D., & Li, Y. (2014). Conversion of strain energy in triaxial unloading tests on marble. *International Journal of Rock Mechanics and Mining Sciences, 66*, 160–168.

Jiang, Q., Su, G., Feng, X., Cui, J., Pan, P., & Jiang, J. (2015). Observation of rock fragment ejection in post-failure response. *International Journal of Rock Mechanics and Mining Sciences, 74*, 30–37.

Karakus, M., Akdag, S., & Bruning, T. (2016). Rock fatigue damage assessment by acoustic emission. In P. Ranjith, & J. Zhao (Ed.), International conference on geo-mechanics, geo-energy and geo-resources, IC3G (pp. 82–88). Melbourne, Australia.

Landis, E., Nagy, E., & Keane, D. (2003). Microstructure and fracture in three dimensions. *Engineering Fracture Mechanics, 70*(7/8), 911–925.

Li, D., Sun, Z., Xie, T., Li, X., & Ranjith, P. (2017). Energy evolution characteristics of hard rock during triaxial failure with different loading and unloading paths. *Engineering Geology, 228*, 270–281.

Li, X., Du, K., & Li, D. (2015). True triaxial strength and failure modes of cubic rock specimens with unloading the minor principal stress. *Rock Mechanics and Rock Engineering, 48*(6), 2185–2196.

Li, Y., Huang, D., & Li, X. (2014). Strain rate dependency of coarse crystal marble under uniaxial compression: Strength, deformation and strain energy. *Rock Mechanics and Rock Engineering, 47*(4), 1153–1164.

Lockner, D. (1993). The role of acoustic emission in the study of rock fracture. *International Journal of Rock Mechanics and Mining Sciences & Geomechanics Abstracts, 30*(7), 883–899.

Meng, Q., Zhang, M., Han, L., Pu, H., & Nie, T. (2016). Effects of acoustic emission and energy evolution of rock specimens under the uniaxial cyclic loading and unloading compression. *Rock Mechanics and Rock Engineering, 49*(10), 3873–3886.

Munoz, H., & Taheri, A. (2017). Specimen aspect ratio and progressive field strain development of sandstone under uniaxial compression by three-dimensional digital image correlation. *Journal of Rock Mechanics and Geotechnical Engineering, 9*(4), 599–610.

Munoz, H., & Taheri, A. (2019). Postpeak deformability parameters of localized and nonlocalized damage zones of rocks under cyclic loading. *Geotechnical Testing Journal, 42*(6), 22p.

Munoz, H., Taheri, A., & Chanda, E. (2016). Pre-peak and post-peak rock strain characteristics during uniaxial compression by 3D Digital Image Correlation. *Rock Mechanics and Rock Engineering, 49*(7), 2541–2554.

Ning, J., Wang, J., Jiang, J., Hu, S., Jiang, L., & Liu, X. (2018). Estimation of crack initiation and propagation thresholds of confined brittle coal specimens based on energy dissipation theory. *Rock Mechanics and Rock Engineering, 51*(1), 119–134.

Okubo, S., Nishimatsu, Y., & He, C. (1990). Loading rate dependence of Class II behaviour in uniaxial and triaxial compression tests: An application of a proposed new control method. *International Journal of Rock Mechanics and Mining Sciences, 27*(6), 559–562.

Peng, R., Ju, Y., Wang, J., Xie, H., Gao, F., & Mao, L. (2015). Energy dissipation and release during coal failure under conventional triaxial compression. *Rock Mechanics and Rock Engineering, 48*(2), 509–526.

Remani, H., & Martin, C. (2018). Cohesion degradation and friction mobilization in brittle failure of rocks. *International Journal of Rock Mechanics and Mining Sciences, 106*, 1–13.

Tarasov, B., & Potvin, Y. (2013). Universal criteria for rock brittleness estimation under triaxial compression. *International Journal of Rock Mechanics and Mining Sciences, 59*, 57–69.

Wawersik, W., & Fairhurst, C. (1970). A study of brittle rock fracture in laboratory compression experiments. *International Journal of Rock Mechanics and Mining Sciences, 7*(5), 561–575.

Weng, L., Huang, L., Taheri, A., & Li, X. (2017). Rockburst characteristics and numerical simulation based on a strain energy density index: A case study of a roadway in Linglong gold mine. *Tunnelling and Underground Space Technology, 69*, 223–232.

Weng, L., Li, X., Taheri, A., Wu, Q., & Xie, X. (2018). Fracture evolution around a cavity in brittle rock under uniaxial compression and coupled static-dynamic loads. *Rock Mechanics and Rock Engineering, 51*(2), 531–545.

Xu, X., & Karakus, M. (2018). A coupled thermo-mechanical damage model for granite. *International Journal of Rock Mechanics and Mining Sciences, 103*, 195–204.

Zhou, C., Xu, C., Karakus, M., & Shen, J. (2019). A particle mechanics approach for the dynamic strength model of the jointed rock mass considering the joint orientation. *International Journal for Numerical and Analytical Methods in Geomechanics, 43*(18), 2797–2815.

Further Reading

Feng, X., Yu, Y., Feng, G., Xiao, Y., Chen, B., & Jiang, Q. (2016). Fractal behaviour of the microseismic energy associated with immediate rockbursts in deep, hard rock tunnels. *Tunnelling and Underground Space Technology, 51*, 98–107.

Peng, J., Rong, G., Cai, M., Yao, M., & Zhou, C. (2016). Physical and mechanical behaviors of a thermal damaged coarse marble under uniaxial compression. *Engineering Geology, 200*, 88–93.